Rapid resistance profiling of SARS-CoV-2 protease inhibitors

Reuben Harris (rsh@uthscsa.edu)
rsh@uthscsa.edu https://orcid.org/0000-0002-9034-9112
Seyed Moghadasi (mogha019@umn.edu)
University of Minnesota
Rayhan Biswas (biswa128@umn.edu)
University of Minnesota https://orcid.org/0000-0002-9656-9175
Daniel Harki (daharki@umn.edu)
University of Minnesota https://orcid.org/0000-0001-5950-931X

Article

Keywords:

DOI: https://doi.org/

Additional Declarations: There is a conflict of interest Competing Interests The Mpro gain-of-signal system is the subject of U.S. Provisional Application Serial No. 63/108,611, filed on November 2, 2020, with RSH and SAM as inventors. The authors declare that there are no additional competing interests.

Brief Communication

Rapid resistance profiling of SARS-CoV-2 protease inhibitors

Seyed Arad Moghadasi[1], Rayhan G. Biswas[1], Daniel A. Harki[1] & Reuben S. Harris[1,2]

[1] University of Minnesota, Minneapolis, Minnesota, USA, 55455

[2] Howard Hughes Medical Institute, University of Texas Health San Antonio, San Antonio, Texas, USA, 78229

Correspondence: mogha019@umn.edu and rsh@uthscsa.edu

Resistance to nirmatrelvir (Paxlovid) has been shown by multiple groups and may already exist in clinical SARS-CoV-2 isolates. Here a panel of SARS-CoV-2 main protease (M^{pro}) variants and a robust cell-based assay are used to compare the resistance profiles of nirmatrelvir, ensitrelvir, and FB2001. The results reveal distinct resistance mechanisms ("fingerprints") and indicate that these next-generation drugs have the potential to be effective against nirmatrelvir-resistant variants and *vice versa*.

Antiviral drugs are necessary to combat SARS-CoV-2/COVID-19, particularly with waning interest in the repeated vaccination boosts necessary to keep-up with virus evolution. The main protease (M^{pro}) of SARS-CoV-2 is essential for virus replication and, accordingly, a proven therapeutic target as evidenced by Paxlovid (active component: nirmatrelvir; **Figure 1A**). However, as for drugs developed to treat other viruses[1] and for first-generation SARS-CoV-2 vaccines, there is a high probability that variants will emerge that resist nirmatrelvir. Indeed, a flurry of recent studies has described a variety of candidate nirmatrelvir-resistance mutations[2-9].

Thus, considerable urgency exists to develop next-generation M^{pro} inhibitors with different resistance mechanisms and, in parallel, robust systems to rapidly assess the potential impact of candidate resistance mutations.

Ensitrelvir (Xocova) and FB2001 are being evaluated in clinical trials, and the former drug also recently received EUA in Japan[10,11] (**Figure 1A**). We recently developed a gain-of-signal system for facile quantification of M^{pro} inhibition[12], and subsequently used it together with an evolution- and structure-guided approach to characterize candidate nirmatrelvir- and ensitrelvir-resistance mutations[2]. Here, an expanded panel of M^{pro} single and double mutants based on recent studies by our group and others[2-9] is leveraged to determine resistance profiles of these two drugs, as well as FB2001, a potential next-generation therapy (heatmap of results in **Figure 1B**; quantification summary in **Table 1**; representative dose responses in **Figure S1**).

Several single amino acid substitution variants including T21I, L50F, P252L, and T304I show minimal resistance to nirmatrelvir, ensitrelvir, or FB2001. Selective resistance to ensitrelvir is conferred by M49I and M49L, whereas selective resistance to nirmatrelvir is caused by A173V (highlighted in gray in **Table 1**). ΔP168 elicits similar resistance to all inhibitors, and synergistic resistance to nirmatrelvir when combined with A173V. S144A and L167F show the greatest resistance to ensitrelvir, intermediate resistance to nirmatrelvir, and lower resistance toward FB2001. In contrast to E166A and L50F/E166A, which cause a similar broad-spectrum resistance, E166V and L50F/E166V elicit very high resistance to nirmatrelvir, intermediate resistance to ensitrelvir, and substantially lower resistance to FB2001.

In addition to providing a method to rapidly profile candidate resistance mutations in living cells, our gain-of-signal assay also provides a quantitative metric for M^{pro} functionality[12] (**Methods**). This system is based on the fact that overexpression of wildtype SARS-CoV-2 M^{pro} results in the cleavage of multiple substrates in cells[13,14] including at least one required for RNA Polymerase II-dependent gene expression[12]. Therefore, expression of the Src-M^{pro}-Tat-Luc reporter itself is rapidly shut down following transfection and can only be recovered by chemical or genetic inhibition of M^{pro}. Thus, genetic mutations effectively phenocopy the chemical dose-responsiveness of the system, with some variations showing wildtype M^{pro} activity (background luminescence) and others compromising activity weakly or strongly depending on the nature of the mutation (low to high luminescence). For example, in comparison to wildtype M^{pro}, catalytic mutants such as C145A yields 50- to 100-fold higher luminescence[2,12]. The M^{pro} variant constructs used here display a range of luminescence levels in the absence of drug indicative of near-normal M^{pro} activity (notably, M49I and M49L), weakly compromised M^{pro} activity (notably, A173V), and strongly compromised M^{pro} activity (notably, E166V) (**Figure S2**). These results suggest that several variants can confer at least partial drug resistance with little loss in M^{pro} functionality (and accordingly high viral fitness), whereas others such as E166V require suppressor mutations such as L50F to restore M^{pro} function to a level that enables virus replication (evidenced by recent resistance studies with pathogenic SARS-CoV-2 in culture and *in vivo* in animal models[3,5]).

Regardless of the details of each molecular mechanism, the results here demonstrate that nirmatrelvir, ensitrelvir, and FB2001 have distinct resistance profiles and that the latter inhibitors (with appropriate formulations) may be effective in patients suffering from Paxlovid rebound[15] or *bona fide* resistance[2]. FB2001 may additionally have a higher resistance barrier given that no fully

functional single M^{pro} variants tested to-date confer a strong resistance to this compound. Importantly, the gain-of-signal live cell assay recapitulates recent findings using replication competent viruses and provides a safe and rapid method for assessing resistance. As the SARS-CoV-2 variant pool deepens, this assay and variant panel can be expanded in lock-step to provide early resistance "fingerprints" of candidate next-generation M^{pro} inhibitors. Such an early profiling strategy has the potential to minimize the risks of developing drugs prone to cross-resistance and, importantly, to help identify inhibitors with the highest barriers to resistance.

Acknowledgments

This work was supported by National Institute of Allergy and Infectious Disease grant U19-AI171954. RSH is an Investigator of the Howard Hughes Medical Institute, a CPRIT Scholar, and the Ewing Halsell President's Council Distinguished Chair at University of Texas Health San Antonio.

Competing Interests

The M^{pro} gain-of-signal system is the subject of U.S. Provisional Application Serial No. 63/108,611, filed on November 2, 2020, with RSH and SAM as inventors. The authors declare that there are no additional competing interests.

Author Contributions

Conceptualization: SAM, RSH; Methodology: SAM, RGB, DAH; Investigation: SAM, RGB; Visualization: SAM; Funding acquisition: RSH; Project administration: RSH; Supervision: RSH, DAH; Writing – original draft: SAM, RSH; Writing – review & editing: All authors

References

1 Majerova, T. & Konvalinka, J. Viral proteases as therapeutic targets. *Mol Aspects Med* **88**, 101159 (2022). https://doi.org:10.1016/j.mam.2022.101159

2 Moghadasi, S. A. *et al.* Transmissible SARS-CoV-2 variants with resistance to clinical protease inhibitors. *Sci Adv* **in press** (2023). https://doi.org:10.1101/2022.08.07.503099

3 Zhou, Y. *et al.* Nirmatrelvir-resistant SARS-CoV-2 variants with high fitness in an infectious cell culture system. *Sci Adv* **8**, eadd7197 (2022). https://doi.org:10.1126/sciadv.add7197

4 Iketani, S. *et al.* Functional map of SARS-CoV-2 3CL protease reveals tolerant and immutable sites. *Cell Host Microbe* **30**, 1354-1362 e1356 (2022). https://doi.org:10.1016/j.chom.2022.08.003

5 Iketani, S. *et al.* Multiple pathways for SARS-CoV-2 resistance to nirmatrelvir. *Nature* **613**, 558-564 (2023). https://doi.org:10.1038/s41586-022-05514-2

6 Jochmans, D. *et al.* The substitutions L50F, E166A, and L167F in SARS-CoV-2 3CLpro are selected by a protease inhibitor in vitro and confer resistance to nirmatrelvir. *mBio*, e0281522 (2023). https://doi.org:10.1128/mbio.02815-22

7 Heilmann, E. *et al.* SARS-CoV-2 3CL(pro) mutations selected in a VSV-based system confer resistance to nirmatrelvir, ensitrelvir, and GC376. *Sci Transl Med* **15**, eabq7360 (2023). https://doi.org:10.1126/scitranslmed.abq7360

8 Noske, G. D. *et al.* Structural basis of nirmatrelvir and ensitrelvir activity against naturally occurring polymorphisms of the SARS-CoV-2 Main Protease. *J Biol Chem*, 103004 (2023). https://doi.org:10.1016/j.jbc.2023.103004

9 Lan, S. *et al.* Nirmatrelvir resistance in SARS-CoV-2 Omicron_BA.1 and WA1 replicons and

escape strategies. *BioRxiv* doi: https://doi.org/10.1101/2022.12.31.522389 (2023).

10 Dai, W. *et al.* Structure-based design of antiviral drug candidates targeting the SARS-CoV-2 main protease. *Science* **368**, 1331-1335 (2020). https://doi.org:10.1126/science.abb4489

11 Unoh, Y. *et al.* Discovery of S-217622, a noncovalent oral SARS-CoV-2 3CL protease inhibitor clinical candidate for treating COVID-19. *Journal of medicinal chemistry* **65**, 6499-6512 (2022). https://doi.org:10.1021/acs.jmedchem.2c00117

12 Moghadasi, S. A. *et al.* Gain-of-signal assays for probing inhibition of SARS-CoV-2 M(pro)/3CL(pro) in living cells. *mBio* **13**, e0078422 (2022). https://doi.org:10.1128/mbio.00784-22

13 Meyers, J. M. *et al.* The proximal proteome of 17 SARS-CoV-2 proteins links to disrupted antiviral signaling and host translation. *PLoS Pathog* **17**, e1009412 (2021). https://doi.org:10.1371/journal.ppat.1009412

14 Gordon, D. E. *et al.* A SARS-CoV-2 protein interaction map reveals targets for drug repurposing. *Nature* **583**, 459-468 (2020). https://doi.org:10.1038/s41586-020-2286-9

15 Anderson, A. S., Caubel, P., Rusnak, J. M. & Investigators, E.-H. T. Nirmatrelvir-ritonavir and viral load rebound in Covid-19. *N Engl J Med* **387**, 1047-1049 (2022). https://doi.org:10.1056/NEJMc2205944

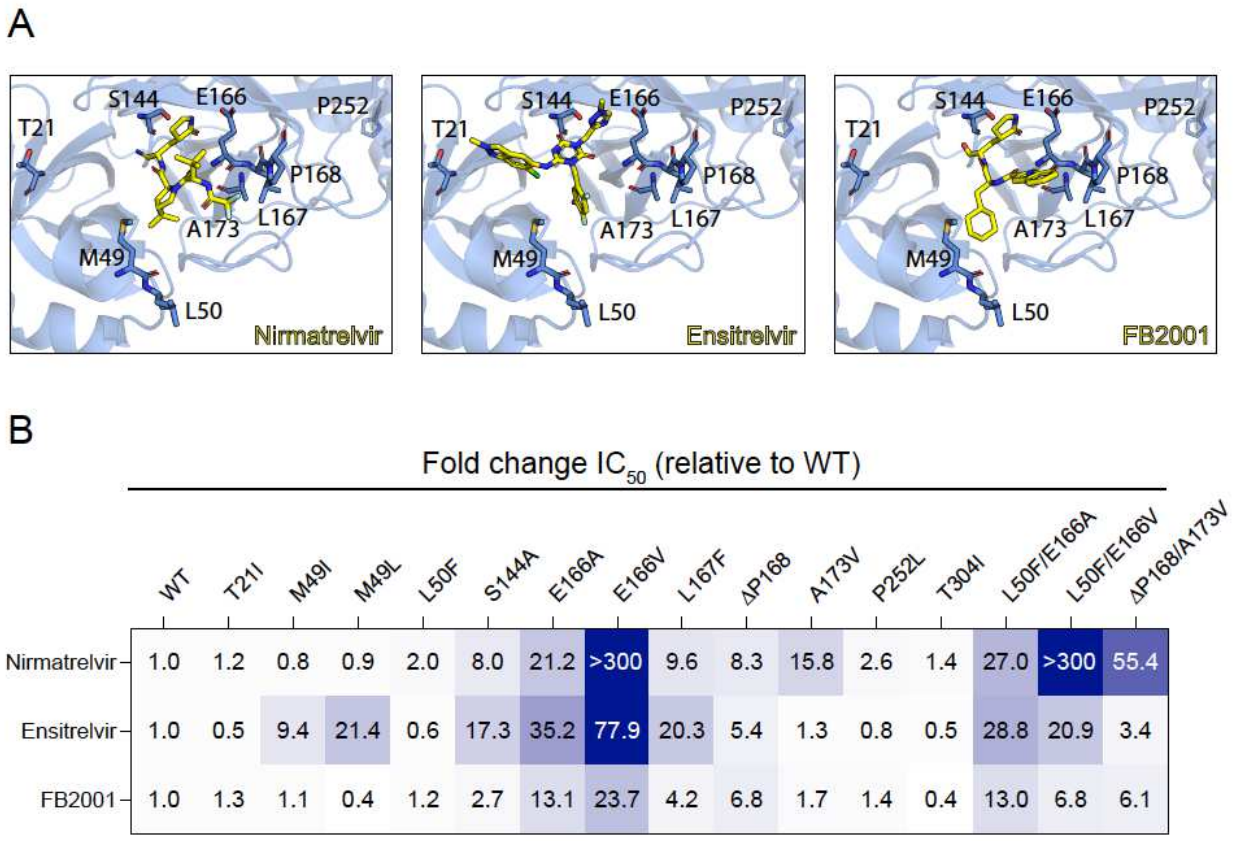

Figure 1. Resistance profiles of nirmatrelvir, ensitrelvir, and FB2001.

(**A**) Co-crystal structures of SARS-CoV-2 M^{pro} in complex with nirmatrelvir (PDB:7SI9), ensitrelvir (PDB:7VU6), or FB2001 (PDB:6LZE). Labeled residues are interrogated in panel B.

(**B**) Fold-change in IC_{50} relative to WT for the indicated mutants using the live cell gain-of-signal assay in 293T cells.

Table 1. IC_{50} values of nirmatrelvir, ensitrelvir, and FB2001 against M^{pro} resistance variants. Clear examples of single amino acid substitution mutations conferring selective resistance to nirmatrelvir and ensitrelvir are highlighted in gray; similar mutations have yet to be found for FB2001. The relative values in brackets are reflected in the heatmap in Figure 1B.

M^{pro} variant	IC_{50} [nM] (Fold-change relative to WT)		
	Nirmatrelvir	**Ensitrelvir**	**FB2001**
WT	29.4 (1.0)	35.9 (1.0)	27.2 (1.0)
T21I	36.0 (1.2)	16.3 (0.5)	34.0 (1.3)
M49I	23.0 (0.8)	338 (9.4)	29.8 (1.1)
M49L	27.1 (0.9)	769 (21.4)	10.7 (0.4)
L50F	58.4 (2.0)	21.0 (0.6)	33.2 (1.2)
S144A	236 (8.0)	623 (17.3)	74.7 (2.7)
E166A	622 (21.2)	126 (35.2)	355 (13.1)
E166V	>10000 (>300)	2800 (77.9)	645 (23.7)
L167F	282 (9.6)	728 (20.3)	115 (4.2)
ΔP168	243 (8.3)	193 (5.4)	184 (6.8)
A173V	460 (15.8)	45.9 (1.3)	45.7 (1.7)
P252L	76.9 (2.6)	28.8 (0.8)	38.9 (1.4)
T304I	40.7 (1.4)	19.0 (0.5)	10.5 (0.4)
L50F/E166A	793 (27)	1040 (28.8)	355 (13)
L50F/E166V	>10000 (>300)	751 (20.9)	185 (6.8)
ΔP168/A173V	1630 (55.4)	122 (3.4)	166 (6.1)

Online Supplementary Information for:

Rapid resistance profiling of SARS-CoV-2 protease inhibitors

Seyed Arad Moghadasi[1], Rayhan G. Biswas[1], Daniel A. Harki[1] & Reuben S. Harris[1,2]

[1] University of Minnesota, Minneapolis, Minnesota, USA

[2] Howard Hughes Medical Institute, University of Texas Health San Antonio, San Antonio, Texas, USA

Correspondence: mogha019@umn.edu and rsh@uthscsa.edu

Contents: Methods and Data Availability, Figures S1 and S2

Methods and Data Availability

Cell culture

All M^{pro} inhibition assays were done as described with the live cell gain-of-signal assay using the pcDNA5/TO-Src-M^{pro}-Tat-fLuc reporter construct[12]. All M^{pro} single and double mutants selected for analysis here were based on recent reports of candidate resistant mutatnts[2-9] generated by site-directed mutagenesis (primers available upon request) and verified by Sanger sequencing. Transfections were done using 293T cells maintained at 37°C and 5% CO_2 in DMEM (Gibco catalog number 11875093) supplemented with 10% fetal bovine serum (ThermoFisher catalog number 11965084) and penicillin-streptomycin (Gibco catalog number 15140122).

M^{pro} resistance experiments

For each individual M^{pro} variant, $3x10^6$ 293T cells were plated in a 10cm dish and transfected 24h later with 2µg of the corresponding variant plasmid using TransIT-LT1(Mirus catalog number MIR 2304). Transfected cells were incubated at 37°C and 5% CO_2 for 4h, washed once with phosphate buffered saline (PBS), trypsinized, resuspended in fresh media, and diluted to a concentration of $4x10^5$ cells/ml. 50µL of each cell suspension was added to a 96-well white clear bottom cell culture plate (ThermoFisher #165306) containing pre-aliquoted inhibitor-supplemented media for a final concentration of 20,000 cells per well and inhibitor dose response range of 10µM to 2.4nM. Inhibitors were purchased from commercial vendors (nirmatrelvir, MedChemExpress catalog number HY-138687; ensitrelvir, MedChemExpress catalog number HY-143216; FB2001, Sigma-Aldrich catalog number SML2877) and purity was confirmed by HPLC and NMR. After an additional 44h incubation (48h total post-transfection), luciferase activity was quantified by removing growth medium and adding 50µL of Bright-Glo reagent (Promega catalog number E2610) to each well and incubating at room temperature in the dark for 2m before measuring luminescence on a Biotek Synergy H1 plate reader.

Percent M^{pro} inhibition was calculated at each concentration of inhibitor using the formula below using the relative luminescence of an inhibitor (RLi) treated sample to the untreated control for each individual mutant.

$$\%\ inhibition = \%100 - (100/(RLi)$$

Results were plotted using GraphPad Prism 9 and fit using a four-parameter non-linear regression to calculate IC_{50} values (**Figure S1**; **Table 1**). Resistance of mutants was calculated by the fold change in IC_{50} of the mutant relative to WT M^{pro}, and these values were used to generate a heatmap

in GraphPad Prism9 (**Figure 1B**).

As an increase in luminescence in the absence of any inhibitor treatment is indicative of decreased M^{pro} catalytic activity, the relative activity of each mutant was calculated by the formula below using the relative luminescence of a mutant (RLm) to the WT enzyme in the absence of inhibitor (**Figure S2**).

$$\%\, activity = \%100 - [100/RLm]$$

Data Availability

All results are presented in the main display items or supplementary figures. The M^{pro} gain-of-signal system is available upon email request to rsh@uthscsa.edu and completion of a MTA (U.S. Provisional Application Serial No. 63/108,611, filed on November 2, 2020).

Ethics

Studies here were performed under University of Minnesota IBC protocol 1902-36822H to RSH, University of Minnesota IBC protocol 2111-39591H to DAH, and University of Texas Health San Antonio IBC B-00000013853 to RSH.

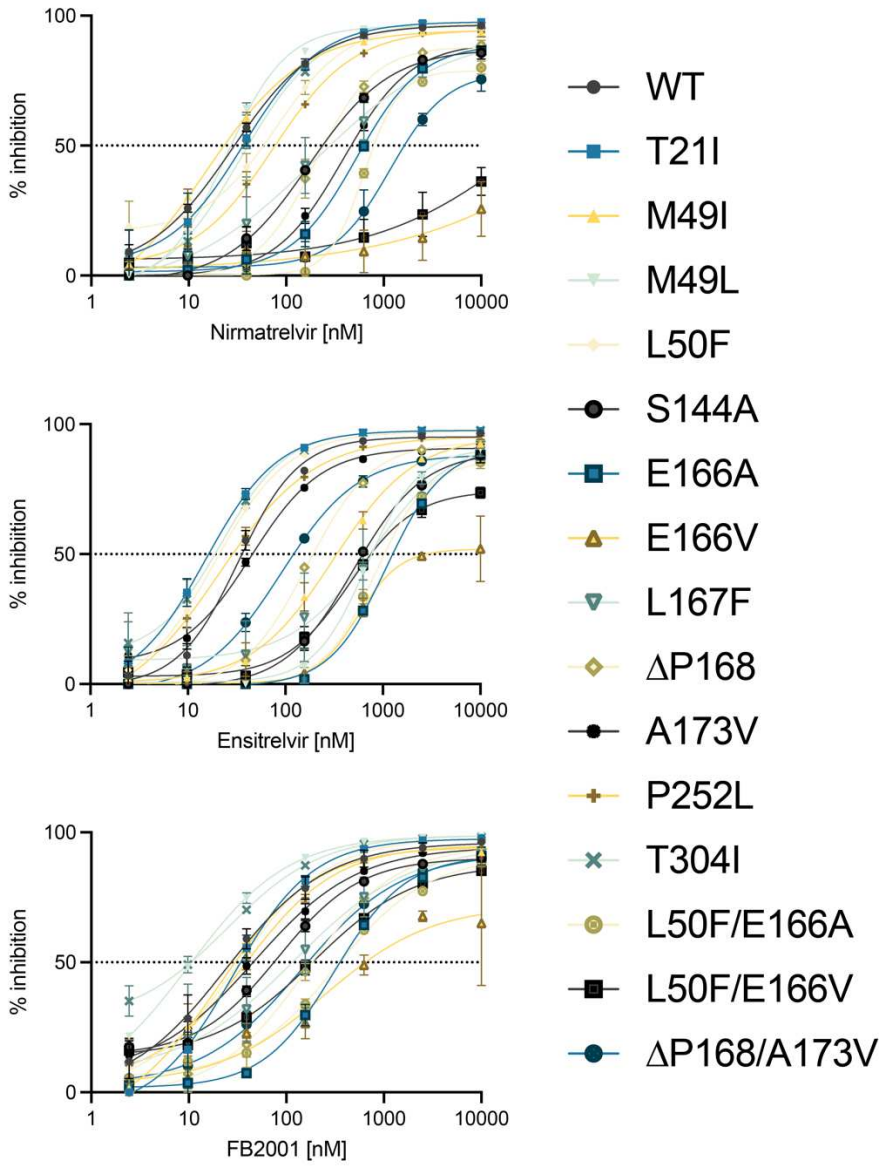

Figure S1. Dose response curves showing inhibition of WT and mutant M^{pro} enzymes by nirmatrelvir, ensitrelvir, and FB2001. Dose response of respective M^{pro} variants using the gain-

of-signal assay in cells treated with indicated inhibitors in a 4-fold serial dilution beginning at 10μM (data are mean +/- SD of biologically independent triplicate experiments). IC_{50} values for each inhibitor are listed in **Table 1**.

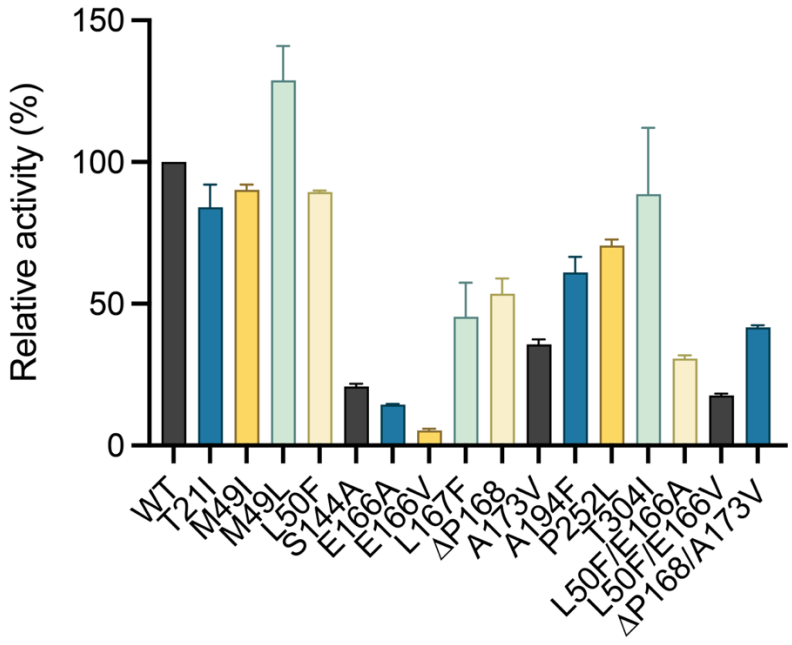

Figure S2. Relative activity of M^{pro} mutants. A histogram showing the relative catalytic activity of each M^{pro} mutant relative to the WT construct (normalized to 100% to facilitate comparison). Several single mutants such as T21I, M49I, M49L, L50F, and T304I show near WT activity. Other mutants such as A173V show modest 1.5 to 3-fold decreases in relative activity, and a few such as E166V are severely compromised. L50F partly restores the activity of E166A and E166V mutants consistent with prior reports[2-9].